11th World Congress on Computational Mechanics (WCCM XI)
5th European Conference on Computational Mechanics (ECCM V)
6th European Conference on Computational Fluid Dynamics (ECFD VI)
E. Oñate, J. Oliver and A. Huerta (Eds)

MULTISCALE TECHNIQUES FOR THE COUPLING OF 3D-1D FSI EQUATIONS SYSTEM IN COMPLIANT VESSELS

D. Cerroni[1], S. Manservisi and F. Menghini

DIN - Laboratory of Montecuccolino, Via dei Colli, 16, 40136 Bologna, Italy.
[1] daniele.cerroni2@unibo.it

Key words: Fluid-structure interaction, incompressible elastic solid and fluid flows, compliant vessel, 3D-1D interface, stabilization method

Abstract. In this paper we present a multiscale model for the analysis of fluid-structure interaction which couples the three-dimensional vessel equations with an appropriate linked mono-dimensional system. This approach allows the study of transient phenomena with remarkable reduction of the computational complexity. This model, when large displacements are taken into account, is of considerable interest for time-dependent simulations of blood flow in components such as large arteries or blood vessels. The computational domain consists of two interacting fluid-structure regions: one described by the multidimensional Navier-Stokes system and the other defined by the structural mechanics equations. Due to the computational cost of fully three-dimensional fluid-structure interaction problems and the complexity of the cardiovascular system, this multi dimensional models can only be applied to selected regions of interest. According to this multiscale approach the rest of the blood circuit is represented by a mono dimensional formulation of the Navier-Stokes system. In particular the mono-dimensional model has to describe properly the wave propagation nature of blood flow and, when coupled with the rest of geometry, must act as a proper absorbing and generating device for the exiting waves inside the computational domain. The mono-three dimensional interface and the multi dimensional geometry of components such as heart valves add complexity to the treatment of inflow and outflow boundaries, where one would like to have a correct representation of the traveling waves, without spurious reflections which may compromise the stability of the solution. In this work we study the propagation of fluid waves into a multidimensional geometry solving fully coupled fluid-structure problem with multiscale approach and present the results of two different cases.

1 INTRODUCTION

In the last decades a great attention has been paid to the study of Fluid-Structure Interaction (FSI) problems because of a large number of applications ranging from bio-medics to civil engineering and aeroelasticity as well. In particular, the numerical solution of the equations of Fluid-Structure Interaction is of great interest from the medical community demanding rigorous and quantitative investigations of cardiovascular diseases. In recent years, the simulation of complex problems in Computational Fluid Dynamics (CFD) has been feasible because of the development of efficient computational techniques and increasing performances of modern computers. However the solution of a Fluid-Structure Interaction problem, when large displacement are taken into account, remains a difficult task.

Several methods have been proposed to deal with moving boundaries in FSI. The most popular one describes the solid motion in a Lagrangian way while an ALE (Arbitrary Lagrangian-Eulerian) formulation is adopted for the fluid [3]. In software packages the segregated approach is the common implemented solution strategy concerning the physical solid-fluid coupling. This method consists of decoupling the problem into separate subproblems over the fluid and solid domains where well-tested numerical solution techniques and efficient solvers are available. Another possibility is to solve implicitly the coupling conditions at each time step leading to a monolithic algorithm. The monolithic algorithm solves simultaneously the fluid and the structure unknowns in a unique solver, so that the solid and fluid regions are treated as a single continuum and the boundary conditions at the interface are automatically taken into account [5, 6].

In most of the cases in the bio-medical applications, the system of interest is a component of the vascular circulatory system and, in order to study the dynamics of that problem, one has to take into account the effect of the entire connected loop. Because of the complexity of the monolithic fully-coupled algorithms, one cannot consider the circulatory system as a unique three dimensional CFD domain, but it is necessary to use multiscale models. In particular we use multidimensional complex model for represent some part of the circulatory system, such as a valve, and a simplified mono-dimensional model for the rest of the loop. The coupling between those modules, multidimensional and mono-dimensional, represents a key topic due to stability issues. In this paper we present the mathematical formulation of the fluid-structure problem in a multiscale framework and introduce appropriate algorithms for solutions. We apply these model in two different cases and present their numerical results.

2 PHYSICS MODEL

2.1 Multidimensional FSI problem

We consider a mechanical system composed by a fluid and a solid domain Ω_t as shown in Figure 1 (see e.g. [3], [13]). Let Ω_t^f and Ω_t^s be the region occupied by the fluid and the solid at the time $t \in (0, T]$, respectively. At the time $t = 0$ the fluid and solid

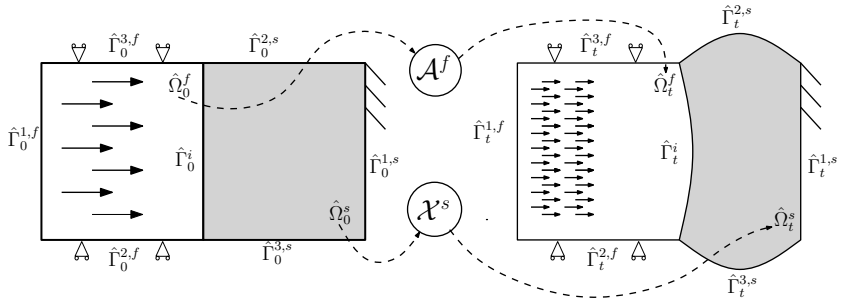

Figure 1: Reference and current configuration where a vessel wall interacts with a fluid.

region are therefore defined by $\hat{\Omega}_0^f$ and $\hat{\Omega}_0^s$. Let $\Gamma_t^i = \bar{\Omega}_t^f \cap \bar{\Omega}_t^s$ and $\hat{\Gamma}_0^i = \bar{\Omega}_0^f \cap \bar{\Omega}_0^s$ be the solid-fluid interfaces and $\Gamma_t^k, k = 1, 2, 3$ and $\hat{\Gamma}_0^k, k = 1, 2, 3$ be the remaining external boundaries, respectively. The evolution of the domain Ω_t can be described by considering the evolution of the solid and fluid parts $\hat{\Omega}_0^f$ and $\hat{\Omega}_0^s$ defined by these two mappings

$$\mathcal{X}^s : \hat{\Omega}_0^s \times \mathbb{R}^+ \to \mathbb{R}^3 \,,$$
$$\mathcal{A}^f : \hat{\Omega}_0^f \times \mathbb{R}^+ \to \mathbb{R}^3 \,,$$

such that $\mathrm{Im}(X^s(\cdot, t)) = \Omega_t^s$, $\mathrm{Im}(\mathcal{A}^f(\cdot, t)) = \Omega_t^f$. The $\mathcal{X}^s$ maps the position of the material point $\hat{\boldsymbol{x}}_0^s$ from the reference configuration $\hat{\Omega}_0^s$ to the current solid material configuration Ω_t^s. The solid displacement is defined as

$$\hat{\boldsymbol{u}}^s(\hat{\boldsymbol{x}}_0^s, t) = \mathcal{X}(\hat{\boldsymbol{x}}_0^s, t) - \hat{\boldsymbol{x}}_0^s \,. \tag{1}$$

The application $\mathcal{A}^f$ is such that $\mathcal{A}^f(\hat{\boldsymbol{x}}_0^f, t) = \hat{\boldsymbol{x}}_0^f + \hat{\boldsymbol{u}}^f(\hat{\boldsymbol{x}}_0^f, t)$, where $\hat{\boldsymbol{u}}^f(\hat{\boldsymbol{x}}_0^f, t)$ is defined as an arbitrary extension over the fluid domain $\hat{\Omega}_0^f$ of the interface solid displacement $\hat{\boldsymbol{u}}^s|_{\hat{\Gamma}_0^i}$

$$\hat{\boldsymbol{u}}^f(\hat{\boldsymbol{x}}_0^f, t) = \mathrm{Ext}(\hat{\boldsymbol{u}}^s|_{\hat{\Gamma}_0^i}) \quad \text{in} \quad \hat{\Omega}_0^f \,. \tag{2}$$

The extension operator $Ext(\cdot)$ commonly used is the harmonic or Laplace operator. This implies that $\hat{\boldsymbol{u}}^f$ is defined by the solution of the elliptic problem

$$\begin{aligned} -k\Delta\hat{\boldsymbol{u}}^f &= 0 \qquad \text{in} \quad \hat{\Omega}_0^f \,, \\ \hat{\boldsymbol{u}}^f &= \hat{\boldsymbol{u}}^s \qquad \text{on} \quad \hat{\Gamma}_0^i \,, \end{aligned} \tag{3}$$

where k is a diffusion coefficient. Other choices for the extension operator can be used, see for instance [12]. Now we can define the velocity $\boldsymbol{w}^f$ of the fluid domain points in the current configuration. The velocity $\hat{\boldsymbol{w}}^f$ is defined by

$$\hat{\boldsymbol{w}}^f = \frac{\partial \hat{\boldsymbol{u}}^f}{\partial t} \quad \text{in} \quad \hat{\Omega}_0^f \,. \tag{4}$$

This quantity represents the velocity in the reference coordinate system $\hat{\boldsymbol{x}}_0^f$ and it is related to $\boldsymbol{w}^f$ by $\hat{\boldsymbol{w}}^f = \boldsymbol{w}^f \circ \hat{\boldsymbol{x}}_0^f$.

The fluid behavior is described by the following incompressible Navier-Stokes equations

$$\begin{aligned}
&\rho^f \frac{\partial \boldsymbol{v}^f}{\partial t}\bigg|_{\tilde{\mathcal{A}}} + \rho^f \left(\boldsymbol{v}^f - \boldsymbol{w}^f\right) \cdot \nabla \boldsymbol{v}^f - \nabla \cdot \boldsymbol{\sigma}^f = \boldsymbol{0} && \text{in} \quad (0,T) \times \Omega_t^f \,, \\
&\nabla \cdot \boldsymbol{v}^f = \boldsymbol{0} && \text{in} \quad (0,T) \times \Omega_t^f \,, \\
&\boldsymbol{v}^f|_{t=0} = \boldsymbol{v}_0 && \text{in} \quad \hat{\Omega}_0^f \,, \\
&\boldsymbol{v}^f|_{\Gamma_{t,D}^{1,f} \cup \Gamma_{t,D}^{2,f}} = \mathbf{g}^f && \text{in} \quad (0,T) \,, \\
&\boldsymbol{\sigma}_f \cdot \boldsymbol{n}^f|_{\Gamma_{t,N}^{1,f} \cup \Gamma_{t,}^{2,f}} = \boldsymbol{h}^f && \text{in} \quad (0,T) \,,
\end{aligned} \tag{5}$$

where ρ^f is the fluid constant density, $\boldsymbol{v}^f$ is the fluid velocity, $\tilde{\mathcal{A}}$ denotes the ALE application that maps the reference fluid configuration $\hat{\Omega}_0^f$ onto the current fluid configuration Ω_t^f and $\boldsymbol{w}^f$ denotes the fluid domain velocity, $\boldsymbol{n}$ is the unit normal vector that points outward from the boundary $\partial\Omega_t^f$ and $\mathbf{g}^f$, $\boldsymbol{h}^f$ and $\boldsymbol{v}_0$ are given data. The variables that determine the state of the flow in the incompressible case are the pressure p^f and the velocity $\boldsymbol{v}^f$. The contribution of external forces like gravity is assumed to be negligible. The constitutive relation for the stress tensor in the Newtonian incompressible case reads

$$\boldsymbol{\sigma}^f = -p^f \boldsymbol{I} + \boldsymbol{\tau}^f = -p^f \boldsymbol{I} + 2\mu^f \boldsymbol{\epsilon}\left(\boldsymbol{v}^f\right) \,, \tag{6}$$

where μ^f is the dynamic viscosity of the fluid, p^f is the Lagrange multiplier associated to the incompressibility constraint and $\boldsymbol{\epsilon}\left(\boldsymbol{v}^f\right)$ is the strain rate tensor defined as

$$\boldsymbol{\epsilon}\left(\boldsymbol{v}^f\right) = \frac{1}{2}\left(\nabla \boldsymbol{v}^f + \left(\nabla \boldsymbol{v}^f\right)^T\right) \,. \tag{7}$$

The material time derivative is related to the adopted reference systems. Three types of reference frames are considered in practice: the Eulerian, the Lagrangian and the Arbitrary Lagrangian-Eulerian frames. In this work we have chosen the ALE formulation which is the most commonly used formulation for Navier-Stokes equations in Fluid-Structure Interaction analysis [4, 10, 9].

The governing equations for structural mechanics are the momentum equations which is, in a Eulerian reference frame, defined by

$$\rho^s \left(\frac{\partial \boldsymbol{v}^s}{\partial t} + \boldsymbol{v}^s \cdot (\nabla \boldsymbol{v}^s)\right) - \nabla \cdot \boldsymbol{\sigma}^s(\boldsymbol{u}^s) = \boldsymbol{0} \qquad \text{in} \quad \Omega_t^s \,, \tag{8}$$

where ρ^s is the density of the material, $\boldsymbol{v}^s$ is the velocity field and $\boldsymbol{\sigma}^s$ is the Cauchy stress tensor, which is a function of the displacement $\boldsymbol{u}^s$ of the structure. Since the constitutive law for the solid stress tensor is expressed in terms of the displacements, one must couple

displacement with velocity. Therefore one must solve the balance equations (8) as a function of the velocity field defined by

$$\boldsymbol{v}^s = \frac{\partial \boldsymbol{u}^s}{\partial t}\,. \tag{9}$$

We notice that from here on the Einstain notation is used so the repeated index imply the summation. For the reference configuration, the right Cauchy-Green tensor, C_{IJ}, is introduced as

$$\boldsymbol{C}_{IJ} = \boldsymbol{F}_{iI}\boldsymbol{F}_{iJ}\,, \tag{10}$$

where $\boldsymbol{F}$ is the deformation gradient tensor that is defined as $\boldsymbol{F} = \boldsymbol{I} + \nabla \boldsymbol{u}^s$. In the current configuration a common deformation measure is the left Cauchy-Green deformation tensor, b_{ij}, expressed as

$$b_{ij} = \boldsymbol{F}_{iI}\boldsymbol{F}_{iI}\,. \tag{11}$$

According with this nomenclature we can now express the Cauchy stress tensor $\boldsymbol{\sigma}^s$ as

$$\boldsymbol{\sigma}^s_{ij} = \frac{2}{J}\begin{bmatrix} b_{ij} & (Ib_{ij} - b_{im}b_{mj}) & \dfrac{J\delta_{ij}}{2} \end{bmatrix} \begin{pmatrix} \frac{\partial W}{\partial I} \\ \\ \frac{\partial W}{\partial II} \\ \\ \frac{\partial W}{\partial J} \end{pmatrix}\,, \tag{12}$$

where $I = \operatorname{tr}\boldsymbol{C}$, $II = \operatorname{tr}(\boldsymbol{C}^2) - (\operatorname{tr}\boldsymbol{C})^2$ are the first and second invariant of the right Cauchy-Green strain tensor $\boldsymbol{C}$ and J its determinant. The quantity $W = W(I, II, J)$ is the strain energy of the system defined by

$$\begin{aligned} W(I,J) &= W^{(1)}(I,J) + \lambda U(J) \\ W^{(1)}(I,J) &= \frac{1}{2}\mu(I - 3 - 2\ln J) + \lambda U(J), \end{aligned} \tag{13}$$

and $U(J)$ by

$$U(J) = \frac{1}{2}(J-1)^2\,. \tag{14}$$

When J is near the unity it may be approximated by

$$J \approx 1 + \frac{\partial u_i}{\partial x_i}\,. \tag{15}$$

At this point we remark that the problem defined by (5) and (8) is not properly posed since we have not prescribed any boundary conditions at the interface Γ^i_t. The coupling

between the fluid and the solid model defines the missing boundary conditions, which imply the continuity of the velocity and the stress field at the interface Γ_t^i as

$$\boldsymbol{v}^f|_{\Gamma_t^i} = \boldsymbol{v}^s|_{\Gamma_t^i}\,, \tag{16}$$

$$\boldsymbol{\sigma}^f \cdot \boldsymbol{n}^f|_{\Gamma_t^i} + \boldsymbol{\sigma}^s \cdot \boldsymbol{n}^s|_{\Gamma_t^i} = \boldsymbol{0}\,. \tag{17}$$

With this assumption the fluid-structure coupled state $(\boldsymbol{v}, p, \boldsymbol{u})$ for a compressible solid and fluid satisfies the following complete set of equations

$$\begin{cases} \rho \frac{\partial \boldsymbol{v}}{\partial t}\Big|_{\tilde{\mathcal{A}}} + \rho\,(\boldsymbol{v}-\boldsymbol{w})\cdot\nabla\boldsymbol{v} + \nabla p - \nabla\cdot\boldsymbol{\tau}^f = \boldsymbol{0} & \text{in} \quad \Omega_t^f \\ \nabla\cdot\boldsymbol{v} = \boldsymbol{0} & \text{in} \quad \Omega_t^f \\ \rho \frac{\partial \boldsymbol{v}}{\partial t}\Big|_{\tilde{\mathcal{X}}} + \nabla p - \nabla\cdot\boldsymbol{\tau}^s(\boldsymbol{u}) = \boldsymbol{0} & \text{in} \quad \Omega_t^s \\ \boldsymbol{v} = \frac{\partial \boldsymbol{u}}{\partial t} & \text{in} \quad \Omega_t^s \\ -k\Delta\boldsymbol{u} = 0 & \text{in} \quad \Omega_t^f \\ \boldsymbol{u}^f = \boldsymbol{u}^s & \text{on} \quad \Gamma_t^i \\ \boldsymbol{w} = \frac{\partial \boldsymbol{u}}{\partial t} & \text{in} \quad \Omega_t^f \end{cases} \tag{18}$$

with the initial conditions

$$\boldsymbol{u}(\hat{\boldsymbol{x}}_0, 0) = \hat{\boldsymbol{u}}_0 \quad \text{in} \quad \hat{\Omega}_0 \tag{19}$$

$$\boldsymbol{v}(\hat{\boldsymbol{x}}_0, 0) = \hat{\boldsymbol{v}}_0 \quad \text{in} \quad \hat{\Omega}_0\,. \tag{20}$$

A variational formulation of the Fluid Structure Interaction equations can be obtained by the usual technique of multiplying (18) by appropriate test functions, performing integrations by parts and taking into account the boundary and interface conditions. This procedure leads to a coupled weak formulation which defines the state variables $\boldsymbol{u} : \hat{\Omega}_t \times [0,T] \to \mathbb{R}^3$, $\boldsymbol{v} : \hat{\Omega}_0 \times [0,T] \to \mathbb{R}^3$, and $p : \hat{\Omega}_t \times [0,T] \to \mathbb{R}$ satisfying the two following coupled nonlinear problems.

The fluid weak-formulation:

$$\begin{aligned} &\frac{d}{dt}\int_{\Omega_t^f} \rho\boldsymbol{v}\cdot\boldsymbol{\phi}\,d\boldsymbol{x} - \int_{\Omega_t^f} \rho(\nabla\cdot\boldsymbol{w})\boldsymbol{v}\cdot\boldsymbol{\phi}\,d\boldsymbol{x} + \int_{\Omega_t^f} \rho_f\,(\boldsymbol{v}-\boldsymbol{w})\cdot\nabla\boldsymbol{v}\cdot\boldsymbol{\phi}\,d\boldsymbol{x} + \int_{\Omega_t^f} p\,\nabla\cdot\boldsymbol{\phi}\,d\boldsymbol{x} \\ &- \int_{\Omega_t^f} \boldsymbol{\tau}^f : \nabla\boldsymbol{\phi}\,d\boldsymbol{x} + \int_{\Omega_t^f} \nabla\cdot\boldsymbol{v}\,\psi\,d\boldsymbol{x} + \int_{\Gamma_{t,N}^f} \boldsymbol{g}_N^f\cdot\boldsymbol{\phi}\,d\boldsymbol{\gamma} - \int_{\Gamma_t^i} (\boldsymbol{\sigma}^f\cdot\boldsymbol{n})\cdot\boldsymbol{\phi}\,d\boldsymbol{\gamma} = 0 \\ &\boldsymbol{v} = \boldsymbol{0} \quad \text{on} \quad \Gamma_{t,D}^f\,, \end{aligned} \tag{21}$$

for all $(\boldsymbol{\phi}, \psi) \in V^f(t)$, where $\boldsymbol{g}_N^f$ is the Neumann boundary condition on the fluid. $\Gamma_{t,N}^f$ is split into two parts which are subsets of Γ_t^1 and Γ_t^2, respectively. On $\Gamma_{t,D}^f$ Dirichlet

boundary conditions are imposed.

The solid weak-formulation:

$$\begin{aligned}
&\frac{d}{dt}\int_{\Omega_t^s}\rho\boldsymbol{v}\cdot\boldsymbol{\phi}\,d\boldsymbol{x}+\int_{\Omega_t^s}p\,\nabla\cdot\boldsymbol{\phi}\,d\boldsymbol{x}-\int_{\Omega_t^s}\boldsymbol{\tau}^s:\nabla\boldsymbol{\phi}\,d\boldsymbol{x}\\
&+\int_{\Omega_t^s}\nabla\cdot\boldsymbol{v}\,\psi\,d\boldsymbol{x}+\int_{\Gamma_{t,N}^s}\boldsymbol{g}_N^s\cdot\boldsymbol{\phi}\,d\boldsymbol{\gamma}-\int_{\Gamma_t^i}(\boldsymbol{\sigma}^f\cdot\boldsymbol{n})\cdot\boldsymbol{\phi}\,d\boldsymbol{\gamma}=0\\
&\boldsymbol{v}=\boldsymbol{0}\quad\text{on}\quad\Gamma_{t,D}^s
\end{aligned}\tag{22}$$

for all $(\boldsymbol{\phi},\psi)\in V^s(t)$, where $\boldsymbol{g}_N^s$ is the Neumann boundary condition on the solid. $\Gamma_{t,N}^s$ denotes the part of Γ_t^1 and Γ_t^2 with Neumann boundary conditions. $\Gamma_{t,D}^s$ is the solid part of the boundary with Dirichlet conditions. Homogeneous Neumann boundary conditions are assumed on the external boundary and therefore the integral surface on $\Gamma_{t,N}^s$ cancels out. For details about the derivation of the variational formulation the interested reader may refer to [11, 4, 10, 9].

By summing the two equations (21-22) the two boundary integrals on the interface cancel out so that the final weak formulation becomes

$$\begin{aligned}
&\frac{d}{dt}\int_{\Omega_t^f}\rho\boldsymbol{v}\cdot\boldsymbol{\phi}\,d\boldsymbol{x}-\int_{\Omega_t^f}\rho(\nabla\cdot\boldsymbol{w})\boldsymbol{v}\cdot\boldsymbol{\phi}\,d\boldsymbol{x}+\int_{\Omega_t^f}\rho_f\,(\boldsymbol{v}-\boldsymbol{w})\cdot\nabla\boldsymbol{v}\cdot\boldsymbol{\phi}\,d\boldsymbol{x}\\
&+\int_{\Omega_t^f}p\,\nabla\cdot\boldsymbol{\phi}\,d\boldsymbol{x}-\int_{\Omega_t^f}\boldsymbol{\tau}^f:\nabla\boldsymbol{\phi}\,d\boldsymbol{x}+\int_{\Omega_t^f}\nabla\cdot\boldsymbol{v}\,\psi\,d\boldsymbol{x}+\int_{\Gamma_{t,N}^f}\boldsymbol{g}_N^f\cdot\boldsymbol{\phi}\,d\boldsymbol{\gamma}\\
&+\frac{d}{dt}\int_{\Omega_t^s}\rho\boldsymbol{v}\cdot\boldsymbol{\phi}\,d\boldsymbol{x}+\int_{\Omega_t^s}p\,\nabla\cdot\boldsymbol{\phi}\,d\boldsymbol{x}-\int_{\Omega_t^s}\boldsymbol{\tau}^s:\nabla\boldsymbol{\phi}\,d\boldsymbol{x}+\int_{\Omega_t^s}\nabla\cdot\boldsymbol{v}\,\psi\,d\boldsymbol{x}+\int_{\Gamma_{t,N}^s}\boldsymbol{g}_N^s\cdot\boldsymbol{\phi}\,d\boldsymbol{\gamma}\,,
\end{aligned}\tag{23}$$

for all $(\boldsymbol{\phi},\psi)\in V(t)$ in the fluid and solid region. Also we must set $\boldsymbol{v}=\boldsymbol{0}$ on $\Gamma_{t,D}^{f,s}$.

2.2 The mono-dimensional FSI model

The mono-dimensional model combines the incompressible Navier-Stokes equation system and a shell model for the vessel walls. This implies that only radial displacements are considered. Under the assumption of axial symmetry of the system we may use a mono-dimensional set of equation. We can integrate (5) with no ALE velocity field over the transverse surface and obtain [1, 13]

$$\begin{cases}
\dfrac{\partial A}{\partial t}+\dfrac{\partial v}{\partial x}=0\,,\\
\dfrac{\partial Q}{\partial t}+\dfrac{\partial}{\partial x}\left(\dfrac{\alpha Q^2}{A}\right)+\dfrac{A}{\rho_f}\dfrac{\partial p}{\partial x}=-2\pi\nu(\alpha+2)\dfrac{Q}{A}\,,
\end{cases}\tag{24}$$

where A is the transverse surface of the system, Q is the flow rate and p the pressure of the system, α the momentum flux correction coefficient, ν the fluid dynamic viscosity and

ρ_f is the fluid density. The system (24) is not closed unless we introduce a constitutive relation for the pressure [1, 13]

$$p = \beta\psi(A) + p_{ref} = \beta\frac{\sqrt{A}}{A_0} - \gamma\frac{\sqrt{A_0}}{A_0}\,, \tag{25}$$

where A_0 is the initial transverse surface of the system with β and γ appropriate coefficient related to the solid Young modulus E. With the area equation (25) the system (24) turns into an hyperbolic closed problem which can be solved by imposing the following appropriate boundary conditions

$$\begin{cases} A = A_0 & \text{on } \Gamma_i \cup \Gamma_o \\ u = u_0 & \text{on } \Gamma_i \\ \partial u/\partial x = 0 & \text{on } \Gamma_o \end{cases}. \tag{26}$$

where Γ_i and Γ_o are the inlet and outlet of the domain, respectively.

The variational formulation of the mono-dimensional problem, is obtained by integrating the system (24) with mono-dimensional weight functions. Briefly one can set $\psi = \psi(s)$ and $\phi = \phi(s)$ assuming that the test functions are only a function of the mono-dimensional coordinate s. This module is properly used for mono-dimensional flows such as channels with single fluid.
Let A be a surface perpendicular to the center-line. Over the surface A we define average density and average velocity as

$$\bar{\rho} = \frac{\int_A \rho\, dA}{A} \qquad \bar{v} = \frac{\int_A \rho\, v\, dA}{\bar{\rho} A}\,. \tag{27}$$

With this definition the first equation of the system (24) becomes

$$\int_0^L \psi(s)\,\frac{\partial}{\partial s}\,(\bar{v})\,ds \;+ \frac{\partial}{\partial t}\,(A)\,ds = \int_0^L \psi(s)\,S_s\,ds \quad \forall \psi \in P(0,L)\,, \tag{28}$$

where S_s is an area deformation source from surface integral.

In a similar way for the average quantities ($\bar{\rho}$, $\bar{v}$, $\bar{p}$), $\bar{Q} = \bar{\rho}\bar{v}A$ and $\phi \approx \phi(s)$ the momentum equation becomes

$$\begin{aligned} &\int_0^L (\frac{\partial}{\partial t}\,\bar{Q})\,\phi(s)\,ds + \int_0^L (\frac{\partial}{\partial s}\,\frac{\bar{Q}^2}{A})\,\phi\,ds = \int_0^L \frac{\partial \bar{p}}{\partial s}\,\phi\,ds \\ &\qquad \int_0^L A\bar{\rho}\mathbf{g}\cdot\widehat{i}_s\,\phi\,ds + \int_0^L \phi(s)\,(M_s + M_v)\,ds \qquad \forall \phi \in V(0,L)\,, \end{aligned} \tag{29}$$

where M_s is from surface integral and M_v from volume contributions. Usually $M_s \approx -\,k\,\frac{\rho}{2}\,\bar{u}|\bar{u}|$ (pressure loss). The volume contribution M_v consists of several terms. It is easy to see that $M_v = M_{v,\tau}(\bar{\tau}) + M_{v,vv}(\bar{\mathbf{v}}\bar{\mathbf{v}} - \bar{v}\bar{v})$ with obvious definition of the terms $M_{v,\tau}$ and $M_{v,vv}$.

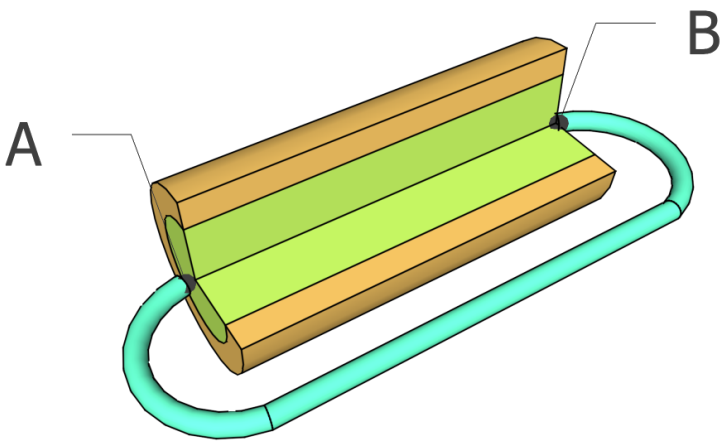

Figure 2: 3D/1D interfaces in a schematic diagram

2.3 3D/1D CFD Interfaces

As shown in Figure 2 the 3D/1D interfaces are the inlet and the outlet of the multi-dimensional regions. The interface between the outlet of the mono-dimensional system and the inlet of the more complex domain is marked with the letter A while the letter B marks the other corresponding interface. Over these interfaces the fluid must flow from one-dimensional module to a three-dimensional one. In this interface the mass and momentum must be conserved. There are many sophisticated techniques to define a numerical algorithm able to identify the values to set on the interfaces for example one can use algorithms based on Mortar or Lagrangian multiplier method [7, 8, 9].

The one-dimensional module is essentially a hyperbolic differential equation and therefore it requires boundary conditions only in inflow regions. The interface 1D/3D-CFD that links the mono-dimensional module to the 3D-CFD module is an outflow region for the system and therefore it does not require boundary conditions. In the inlet region of the multi-dimensional system therefore the average velocity must be set as boundary conditions. This is a very challenging situations since from the mono-dimensional loop we have the propagation of mass flux Q (or velocity in the normal direction) and cross section area A. In three-dimensional domains if the velocity vector is fully specified on boundaries then the pressure is determined so it can be specified only if the normal component of the velocity field is not imposed. Imposing time dependent pressure value on the inlet surface leads to large oscillations and velocity discontinuities. For this reason the pressure is expressed as a function of the cross section dimension so that we avoid the coupling between the two systems pressure values and obtain the continuities of this field by imposing a fixed cross section dimension at the boundary of the system.

3 NUMERICAL RESULTS FOR TEST 1

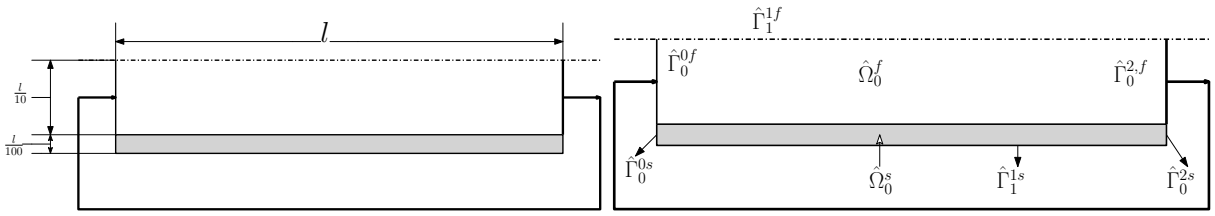

Figure 3: Test 1. Geometry (left) and boundary condition (right).

Physical parameters	**Fluid**	**solid**	Units
Poisson module	–	0.5	–
Young module	–	400000	Pa
Viscosity	1	–	$\mathrm{Pa}\cdot\mathrm{s}$
Density	1000	1000	$\mathrm{kg\ m^{-3}}$

Table 1: Test 1. Physical parameters of the numerical simulation.

In this test we consider a pipe type system coupled with a mono-dimensional one in which a main component moves a certain mass and re-inject the flow periodically. In Figure 3 the geometry of the system is shown and we can appreciate that we consider an axial symmetric system with $l = 1.5m$, radius $r = 0.15m$ and thickness $s = 0.015m$. With reference on the labels shown in Figure 3 the boundary conditions imposed for the fluid ($\hat{\Omega}^f$) are

$$\begin{cases} u_1 = u_m & \text{on } \hat{\Gamma}_0^{0,f}\,, \\ u_2 = 0 & \text{on } \hat{\Gamma}_0^{0,f}\,, \\ \frac{\partial u_i}{\partial x_i} = 0, & \text{on } \hat{\Gamma}_0^{2,f} \quad i = \{1,2\}\,, \\ \frac{\partial u_1}{\partial x_2} = 0 & \text{on } \hat{\Gamma}_1^{1,f}\,, \\ u_2 = 0, & \text{on } \hat{\Gamma}_1^{1,f}\,, \end{cases} \tag{30}$$

where u_m is the velocity coming from the mono-dimensional system. For the solid domain ($\hat{\Omega}^s$) the boundary conditions becomes

$$\begin{cases} u_1 = 0 & \text{on } \hat{\Gamma}_0^{0,s} \cup \hat{\Gamma}_0^{2,s}\,, \\ \frac{\partial u_2}{\partial x_2} = 0, & \text{on } \hat{\Gamma}_0^{0,s} \cup \hat{\Gamma}_0^{2,s} \cup \hat{\Gamma}_1^{1,s} \quad i = \{1,2\}\,, \\ \frac{\partial u_1}{\partial x_2} = 0 & \text{on } \hat{\Gamma}_1^{1,s}\,. \end{cases} \tag{31}$$

The fluid physical parameters are $\mu^f = 2\,\mathrm{Pa}\cdot\mathrm{s}$ and $\rho^f = 1000\,\mathrm{kg/m^3}$, whereas for the solid we have $\rho^s = 1000\,\mathrm{kg/m^3}$, $E = 400000\,\mathrm{Pa}$ and $\nu = 0.5$. These parameters are summarized in Table 1.

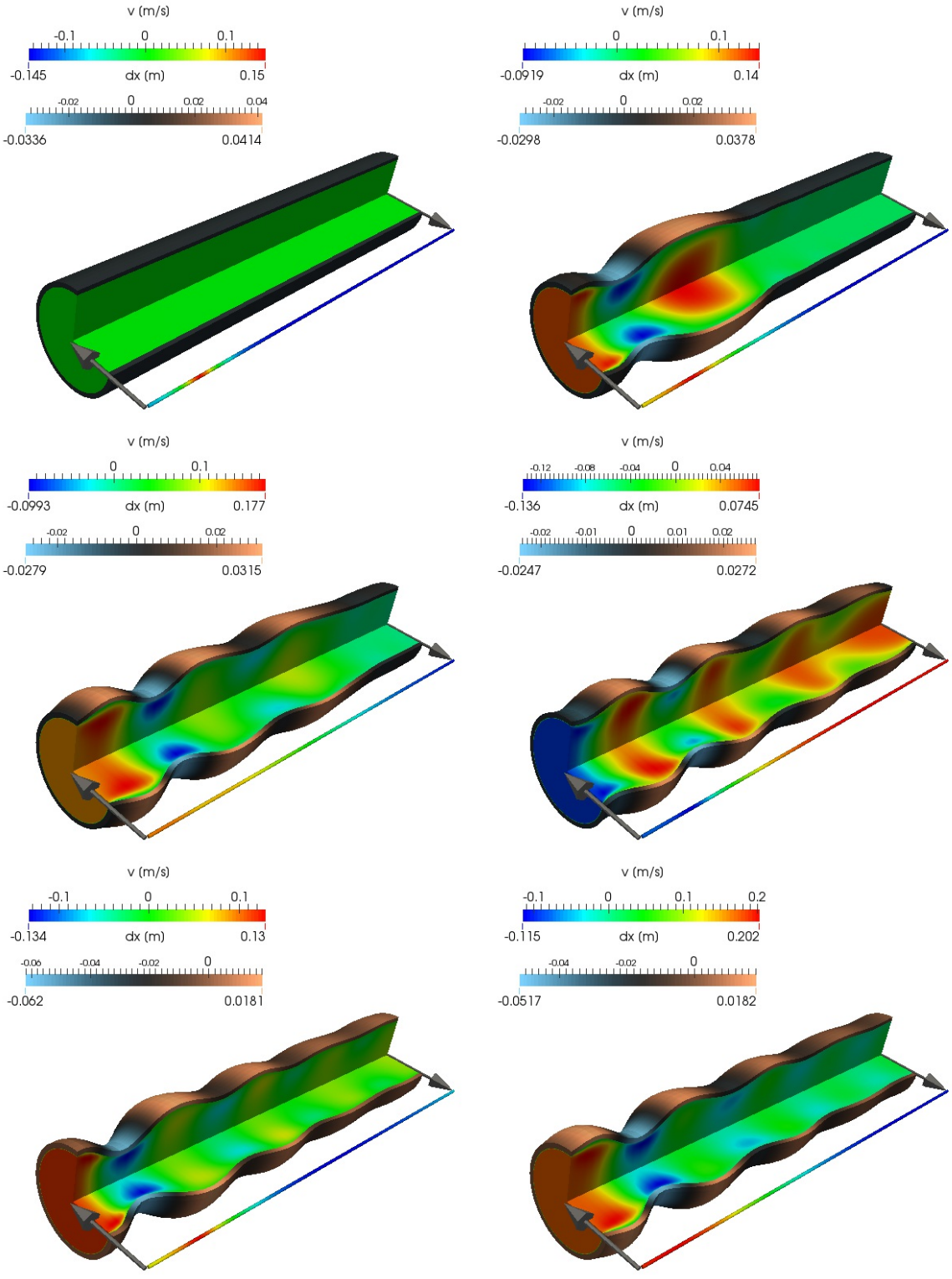

Figure 4: Test 1. Overview displacement velocity field at $t = 0$, 2, 4, 6, 8 and $10s$

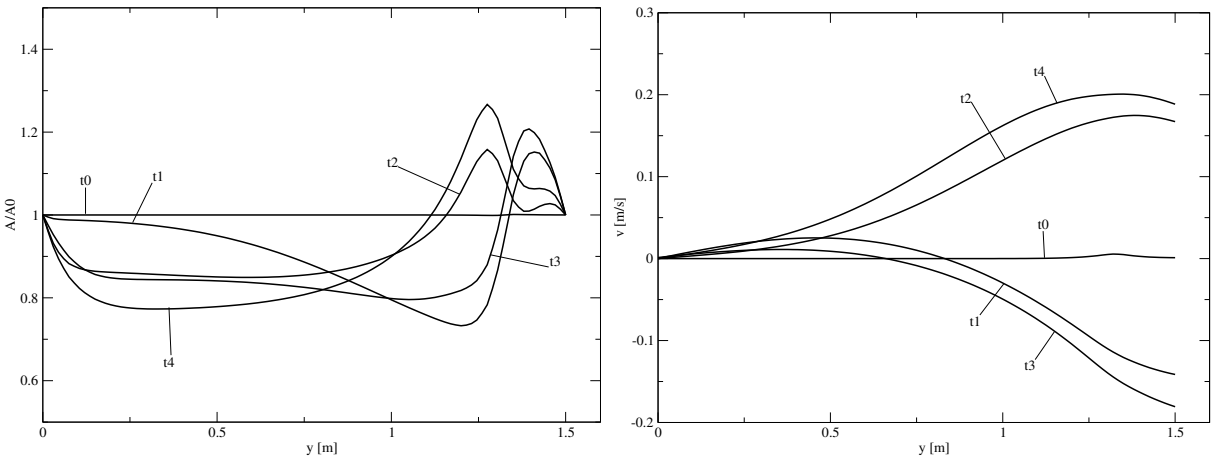

Figure 5: Test 1. Cross section dimension (left) and velocity field (right) in the mono-dimensional system at $t = 0$ (t_0), 2 (t_1), 4 (t_2), 6 (t_3) and 8 (t_4) sec.

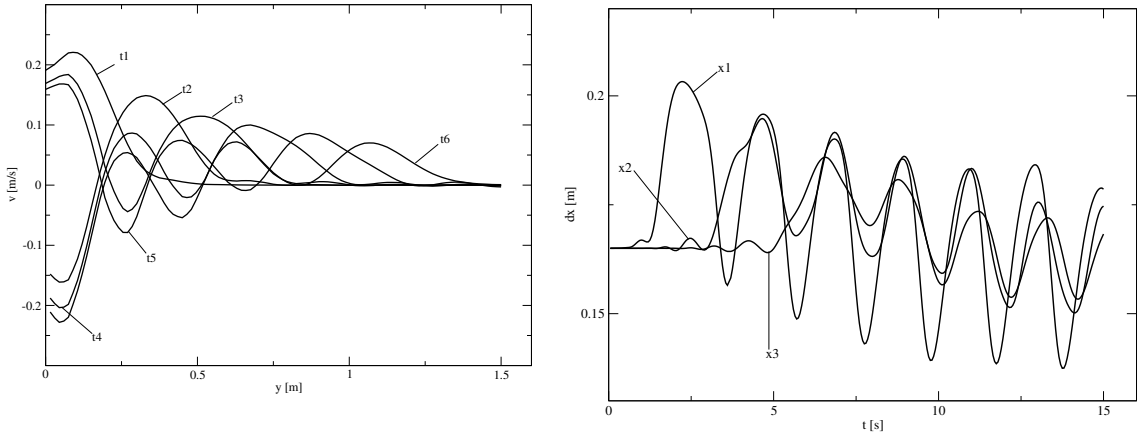

Figure 6: Test 1. Axial velocity in fluid domain at $t = 2$ (t_1), 4 (t_2), 6 (t_3), 8 (t_4), 10 (t_5) and 12 (t_6) sec (left) and displacement field over time in solid domain in $x_1 = (0.165, 0.375)[m]$, $x_2 = (0.165, 0.75)[m]$ and $x_3 = (0.165, 1.125)[m]$ (right).

In Figures 4 the fluid velocity field and the solid displacement are shown at $t = 0$, 2, 4, 6, 8 and 10 sec. We can clearly see the propagation and the attenuation of the displacement wave through the three-dimensional domain. In Figure 5 on the left the cross section A is plotted against the spatial coordinate and the mono-dimensional velocity at different time $t = 0$, 2, 4, 6 and $8s$ is shown on the right. We can remark that the ratio A/A_0 never reaches values lower than 0.7, and the velocity field oscillates inside the interval $[-0.2, 0.2]\, m/s$. In Figure 6 on the left the axial fluid velocity ($x = 0.25m$) is plotted at different time $t = 2$ (t_1), 4 (t_2), 6 (t_3), 8 (t_4), 10 (t_5) and 12 (t_6) sec. In a similar way on the right of Figure 6 the displacement field is shown over time at different points of the solid domain. The considered points are set at $(0.165, 0.375)$, $(0.165, 0.75)$ and

$(0.165, 1.125)$ and labeled by x_1, x_2 and x_3, respectively. From the first plot we can see the time variation of the inlet velocity and his space propagation. In the plot on the right we can observe the delay of the deformation wave at different points and its dumping due to the viscosity of the fluid.

4 NUMERICAL RESULTS FOR TEST 2

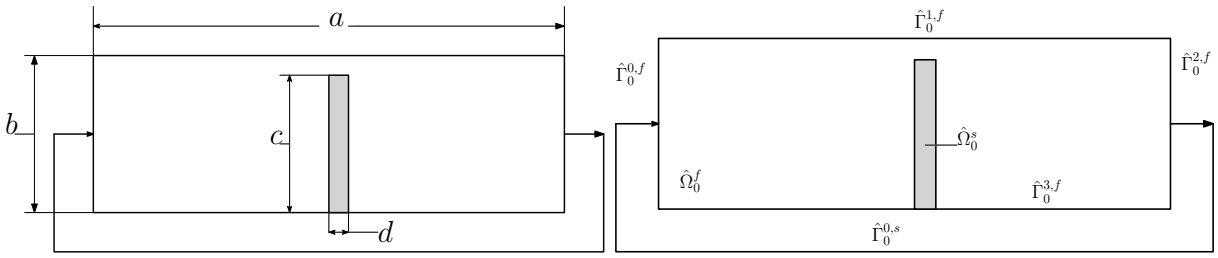

Figure 7: Test 2. Geometry domain and boundary conditions.

Physical parameters	**Fluid**	**solid**	Units
Poisson module	–	0.5	–
Young module	–	400000	Pa
Viscosity	1	–	$\mathrm{Pa} \cdot \mathrm{s}$
Density	1000	1000	$\mathrm{kg\ m^{-3}}$

Table 2: Test 2. Physical parameters of the numerical simulation.

In the second test we consider a fluid channel in which a thin solid plate bends to the fluid motion. In this case the physical dynamics of the mono-dimensional system is analogous to the previous case. In Figure 7 (left) the geometry of the problem is shown, in particular for our case we consider $a = 1.5m$, $b = 0.5m$, $c = 0.45m$ and $d = 0.01m$. According to the labels defined in Figure 7 (right) the boundary conditions of the problem are set as

$$\begin{aligned} &u_1 = u_m, && \text{on } \in \hat{\Gamma}_0^{0,f} \\ &u_2 = 0 && \text{on } \hat{\Gamma}_0^{0,f} \\ &u_i = 0 && \text{on } \hat{\Gamma}_0^{1,f} \cup \hat{\Gamma}_0^{3,f} \quad i = \{1,2\} \\ &\frac{\partial u_i}{\partial x_i} = 0 && \text{on } \hat{\Gamma}_0^{2,f} \quad i = \{1,2\} \\ &u_i = 0 && \text{on } \hat{\Gamma}_0^{0,s} \quad i = \{1,2\}\ . \end{aligned} \tag{32}$$

The fluid physical parameters are $\mu^f = 1\,\mathrm{Pa} \cdot \mathrm{s}$ and $\rho^f = 1000\,\mathrm{kg/m^3}$, whereas for the solid we have $\rho^s = 1000\,\mathrm{kg/m^3}$, $E = 400000\,\mathrm{Pa}$ and $\nu = 0.5$. These parameters are

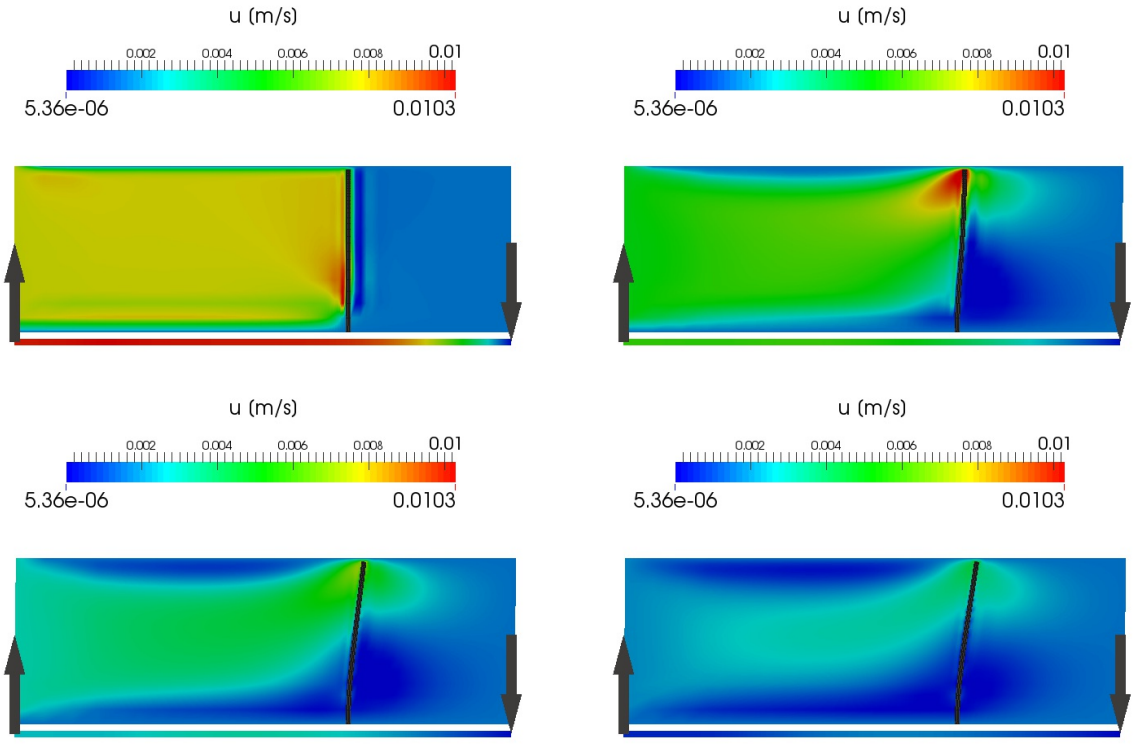

Figure 8: Test 2. Overview of the velocity field at $t = 1$, 2, 3 and 4 sec.

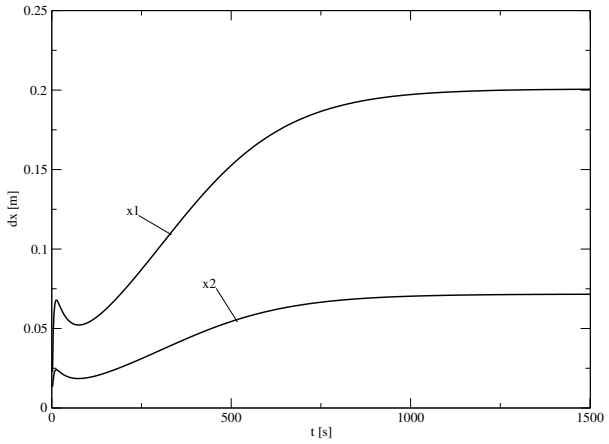

Figure 9: Test 2. Overview of the displacement as a function of time at $x_1 = (1,005\,,\,0.45)[m]$ and $x_2 = (1,005\,,\,0.2)[m]$.

summarized in Table 2. In Figures 8 the fluid velocity field is shown at $t = 1$, 2, 3 and 4 sec. In Figure 9 the displacement of two different points of the solid domain is plotted. In particular we consider the points $x_1 = (1,005\,,\,0.45)[m]$ and $x_2 = (1,005\,,\,0.2)[m]$ which

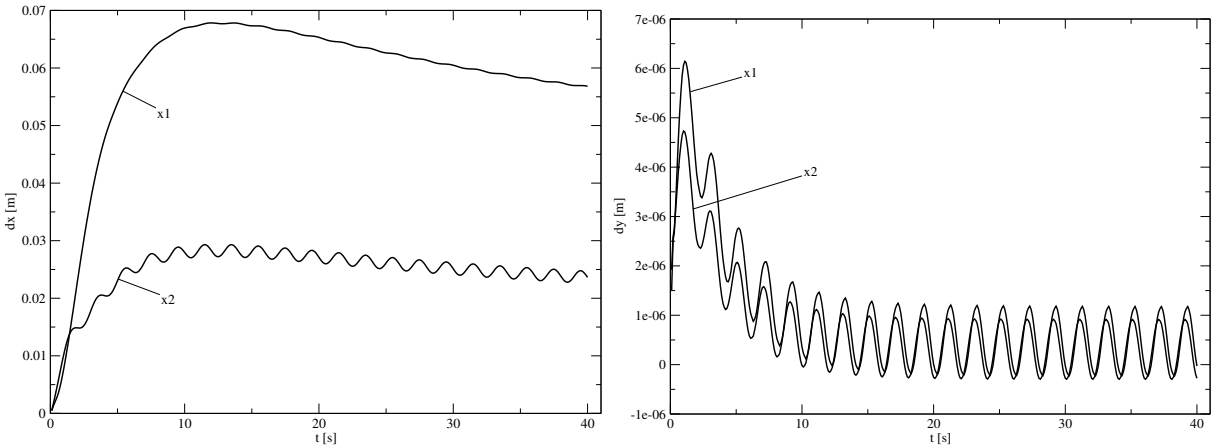

Figure 10: Test 2. Displacements as a function of time in the x direction (left) and in the y direction (right) at $x_1 = (1,005\,,\, 0.45)[m]$ and $x_2 = (1,005\,,\, 0.2)[m]$

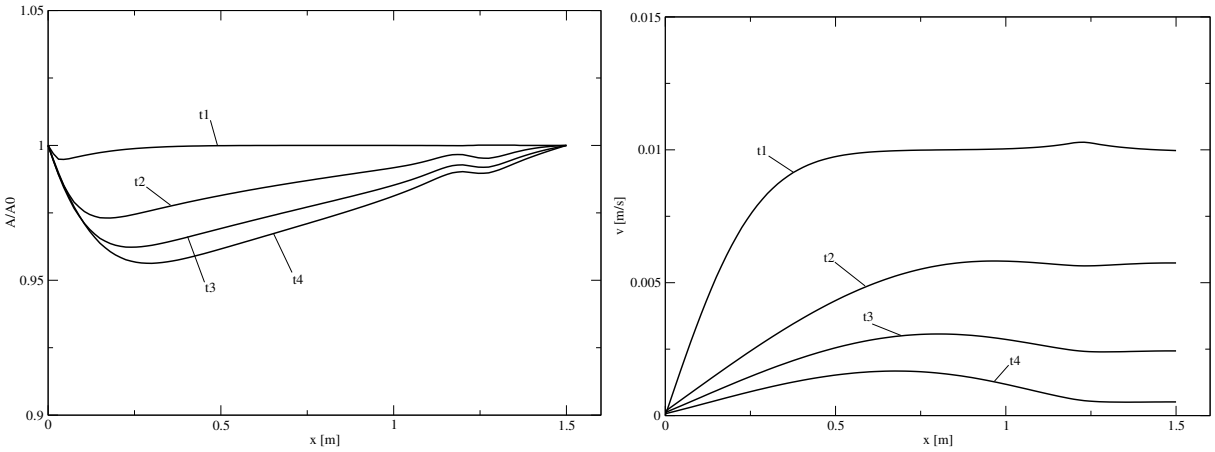

Figure 11: Test 2. Cross section length (left) and the velocity field (right) in the mono-dimensional system at different time $t = 1$ (t_1), 2 (t_2), 3 (t_3) and 5 (t_4) sec.

are located at the top and in the middle of the solid domain, respectively. We can see that the value of the displacement equal to $0.19m$ for x_1 and $0.06m$ for x_2 are reached after about $1000s$. In Figure 10 a detailed view is provided in order to describe the behavior of the solid displacement. In particular on the left of Figure 10 the displacement along the x-axis (dx) is shown while on the right one can see the y-axis displacement (dy). We can clearly see that the fluctuations, due to the mono-dimensional system source term, have a frequency of about $2s$. Finally in Figure 11 the main cross section dimension of the area A (on the left) and the velocity field (on the right) are shown at different $t = 1$ (t_1), 2 (t_2), 3 (t_3), 5 (t_4) sec. and different spatial locations. In particular one can clearly see that the ratio A/A_0 does not reach values lower than 0.95.

5 CONCLUSIONS

In this paper we have analyzed two problems for testing the coupling of a mono-dimensional with a 3D/2D Fluid Structure Interaction system. The first test consists of a multidimensional FSI system linked to a mono-dimensional deformable external loop. In the second test a solid plate bends inside a fluid channel driven by a time dependent coupled mono-dimensional external system. All the results have shown a great stability reached by using a finite element monolithic approach which couples the interface through the velocity field.

REFERENCES

[1] E. Oñate and M. Cervera, *Derivation of thin plate bending elements with one degree of freedom per node*, Engng. Comput., Vol. 10, pp. 543–561 (1993).

[2] O.C. Zienkiewicz and R.L. Taylor, *The Finite Element Method*, Sixth Edition, Elsevier, New York (2005).

[3] J. Donea, S. Giuliani and J. Halleux, *An Arbitrary Lagrangian Eulerian Finite Element Method for transient Fluid-Structure Interactions*, Comput. Meth. Appl. Mech. Eng., Vol. 33, pp. 689–723 (1982).

[4] S. Bna, G. Bornia, S. Manservisi, *A penalty-projection algorithm for incompressible fluid-structure interaction*, Proceedings of the 6th European Congress on Computational Methods in Applied Sciences and Engineering (ECCOMAS 2012), September 10-14, 2012, Vienna, Austria, (J. Eberhardsteiner, H.J. Bohm, F.G. Rammerstorfer), Vienna Uni- versity of Technology, Austria, ISBN: 978-3-9502481-9-7 (2012) 6472-6491

[5] J. Hron and S. Turek, *A Monolithic FEM Solver for an Ale Formulation of Fluid-Structure Interaction with configuration for numerical benchmarking*, European Conference on Computational Fluid Dynamics (P. Wesseling, E. Onãte, and J. Périaux eds.), (2006).

[6] M. Heil, *An Efficient Solver to the Fully Coupled Solution of Large-Displacement Fluid-Structure Interaction Problems*, Comput. Meth. Appl. Mech. Eng., Vol **193**, 1-23 (2004).

[7] E. Aulisa, A. Cervone, S. Manservisi and P. Seshaiyer, *A multilevel domain decomposition approach for studying coupled flow applications*, Commun. Comput. Phys., Vol. 6, pp. 319-341 (2009).

[8] E.Aulisa, S. Manservisi and P. Seshaiyer, *A multilevel domain decomposition approach to solving coupled applications in computational fluid dynamics*, International Journal for Numerical Methods in Fluids, Vol. 56/8, pp. 1139-1145 (2008).

[9] E. Aulisa, S. Manservisi and P. Seshaiyer, *computational multilevel approach for solving 2D Navier-Stokes equations over non-matching grids*, Computer Methods in Applied Mechanics and Engineering, Vol. 195/33-36, pp. 4604-4616 (2006).

[10] E. Aulisa, S. Manservisi and P. Seshaiyer, *A non-conforming computational methodology for modeling coupled problems*, Nonlinear Analysis, Vol. 63, 1445-1454 (2005).

[11] L. Formaggia, A. Quarteroni and A. Veneziani, *Cardiovascular Mathematics*, Springer, New York (2009).

[12] P.A. Sackinger, P.R. Schunk and R.R. Rao, *A Newton-Raphson pseudo-solid domain mapping technique for free and moving boundary problems: a finite element implementation*, Journal of Computational Physics, Vol. 125(1), pp. 83-103 (1996).

[13] P. Le Tallec, and J. Mouro, *Fluid structure interaction with large structural displacements*, Computer Methods in Applied Mechanics and Engineering, Vol. 190(24-25), pp. 3039-3067 (2001).